Scripta Materialia 146 (2018) 236–240

Contents lists available at ScienceDirect

Scripta Materialia

journal homepage: www.elsevier.com/locate/scriptamat

Regular article

Correlating micro-pillar compression behavior with bulk mechanical properties: Nanolaminated graphene-Al composite as a case study

Yihui Hu, Qiang Guo *, Lei Zhao, Zan Li, Genlian Fan, Zhiqiang Li, Ding-Bang Xiong, Yishi Su, Di Zhang *

State Key Lab of Metal Matrix Composites, Shanghai Jiao Tong University, 800 Dongchuan Road, Shanghai 200240, China

ARTICLE INFO

Article history:
Received 29 October 2017
Accepted 2 December 2017
Available online xxxx

Keywords:
Metal matrix composites
Nanolaminated structure
Graphene
Compression test
Size effect

ABSTRACT

Uniaxial compression tests were carried out on nanolaminated graphene (reduced graphene oxide, RGO)-Al composite micro-pillars of various diameters. It was found that, when the pillar diameter was an order of magnitude larger than the internal microstructural length scale (Al lamella thickness), the pillars' mechanical behavior resembled that of the corresponding bulk. When the external length scale approached the internal one, however, both mechanical strength and deformation mode of the pillars significantly deviated from their bulk behavior. These results may have implications for the dimensional design of the small scale test specimens fabricated from bulk materials with a "real" microstructure.

Recent development of micro-/nano-mechanical characterization on small scale specimens provides powerful new tools for probing some of the materials properties that were once unattainable by conventional experimental methods [1,2]. In these studies, micro-/nano-scaled test specimens are fabricated by focused ion beam (FIB) milling [2] or a lithography-based method [3], and are then subject to uniaxial tension or compression. The resulting stress vs. strain response, combined with ex situ [3] or in situ [4] site-specific microstructral analysis, contains important information for the rich interplay between various crystal defects (such as dislocations) in the specimen interior and the sample free surface. These measurements have been widely applied in the study of single crystals [5], bi-crystals [6,7], polycrystals [8–10], alloys [11], amorphous metals [12], and engineering composites [13], and are found to be especially useful for studying the mechanical behavior of thin film-typed samples which would otherwise solely rely on the use of nanoindentation [14,15]. In addition, in micro-/nano-mechanical tests, a single interface (or boundary) can be isolated in the test specimens [7,16,17], so that the properties and effects of the particular boundary can be pinpointed.

Despite the above-mentioned capability of micro-/nano-scaled mechanical characterization techniques, caution has to be exercised if one attempts to interpret *bulk* materials properties using the micro-/nano-mechanical data, as both mechanical strength and flow behavior may show notable size effect when the dimension of the material is reduced to small scales [18,19]. This is particularly true when both *external* and *internal* microstructural length scales are present and are of comparable magnitudes in the test specimens, for example in the case of nanocrystalline [10,20] and nanolaminated [21–23] micro-/nano-pillars, where the overall mechanical behavior of the pillars is determined by the competition of the two length scales [18]. Therefore, to correctly extrapolate bulk behavior from micro-/nano-mechanical test results and offer insights for the deformation mechanism of real, engineering materials, careful design on the specimen dimension is a necessity, so that the micro-/nano-scaled sample is *large enough* to still properly reflect macroscopic materials properties, and is also *small enough* to be processed within reasonable timeframe and experimental effort.

In this context, this study provides a thorough survey on the size-dependent mechanical behavior of micro-/nano-pillars fabricated from bulk nanolaminated graphene (reduced graphene oxide, RGO)-pure Al composite [24], with the aim of correlating micro-/nano-mechanical test data with the corresponding macroscopic material behavior. The RGO-Al composite [13,24] serves as an ideal model material for this purpose in the sense that it not only has excellent bulk tensile properties which make them promising for structural applications, but also possesses an ordered nanolaminated structure that allows accurate control over the microstructural features existing in the small scale test specimens [13]. Specifically, in this study, the stress vs. strain response and deformation mechanism of the pillars of varying diameters were examined. It was found that, above a certain size, the pillars' mechanical behavior resembled that of the corresponding bulk while in the smaller pillar size group where the external length scale approached the internal one, both the mechanical strength and the deformation mode of the pillars significantly deviated from their bulk behavior. These results may have implications for the dimensional design of the small scale test specimens fabricated from bulk materials with a "real" microstructure.

Bulk nanolaminated RGO-Al composite with 1.50 vol% RGO concentration was fabricated by a modified powder metallurgy route [24,25].

* Corresponding authors.
E-mail addresses: guoq@sjtu.edu.cn (Q. Guo), zhangdi@sjtu.edu.cn (D. Zhang).

https://doi.org/10.1016/j.scriptamat.2017.12.004
1359-6462/

The resulting Al lamella thickness was around 200 nm, and the lamella interface was comprised of a few (<10) RGO layers sandwiched between ~5 nm thick amorphous alumina layers grown on the surface of two adjacent Al lamellas. These amorphous alumina layers were likely to have formed during the fabrication process as a result of the easy oxidation of Al surface. Details of the fabrication of RGO-Al composites and their microstructural characterization were described in Refs [24,25].

Cylindrical pillars of varying diameters [diameter (D) = 0.5 μm, 1 μm, 1.5 μm, 2 μm, and 3 μm] with an aspect ratios of ~4:1 were fabricated from the polished rolling surface of the bulk composite sample using a dual beam FIB system (FEI Scios), which also allows scanning electron microscopy (SEM) imaging. The nanolaminates were oriented in parallel with the pillar axis ("0° pillars", Fig. 1b inset), in the *same* isostrain configuration as the bulk composite specimens used in macroscopic tensile test [13]. The vertical taper of pillars larger than 0.5 μm-diameter was controlled within 2°, and the taper of the 0.5 μm-diameter pillars may become as high as 3°. For each pillar size group, >10 pillars were fabricated to get reliable statistics in the following mechanical test. Uniaxial compression on the pillars were conducted using an Agilent G200 nanoindenter equipped with a 15 μm-diameter flat punch diamond tip at room temperature, at a nominally constant strain rate of 0.005 s^{-1}, and to a maximum strain of 10%. The diameters of the as-fabricated pillars were measured from SEM images at half pillar height. True stress–strain curves were employed to characterize the deformation behavior following the methodology developed by Greer et al. [3]. The morphology of the pre- and post-compression pillars was examined by SEM, and their microstructural features were characterized by site-specific TEM analysis where the TEM specimens were prepared using FIB.

Fig. 1(a) shows representative uniaxial compressive stress vs. strain responses for RGO-Al micro-pillars of varying diameters. The yield strengths (σ_y) of 1 μm-, 1.5 μm-, 2 μm-, and 3 μm-diameter were measured to be 425 ± 20 MPa, 431 ± 59 MPa, 395 ± 81 MPa and 415 ± 51 MPa, respectively, showing little variation over pillar size. An abrupt softening took place at the D = 0.5 μm pillar size, and σ_y was considerably reduced to 275 ± 38 MPa. For pillars showing discontinuous flow behavior (D = 0.5 μm, 1 μm, 1.5 μm, and 2 μm), σ_y [as arrowed in Fig. 1(a)] was identified as the stress at the first discrete displacement burst that occurred post-1% strain in each curve, and a threshold of $\Delta\varepsilon \geq 0.002$ was used to identify the burst events [26]. For pillars with smooth stress vs. strain response (D = 3 μm), the conventional 0.2% proof stress was used as σ_y. The size dependence of pillar strength can be more clearly appreciated in Fig. 1(b), where the average yield strength (~410 MPa) for pillars of D = 1 μm, 1.5 μm, 2 μm and 3 μm was indicated by a dotted line.

Fig. 1(a) also demonstrates that the compressive flow behavior differs greatly for composite pillars of different sizes. In particular, pillars of larger diameters possessed smoother stress vs. strain response, as opposed to the intermittent deformation characteristic of their smaller counterparts. Previous studies on the mechanical behavior of micro-/nano-pillars suggest that such jerky plastic flow is correlated with the avalanche of dislocations in small-scale crystals and their annihilation at the internal boundaries and/or free sample surfaces [5,27]. A quantitative evaluation was done by measuring the size of the discrete burst (using the stress burst increment in ascending section of each burst as the benchmark [13,28]) on the stress vs. strain curves as a function of pillar diameter. The results are documented in Table 1, where it is clearly shown that the burst size decreased in a monotonic manner with increasing pillar diameter, from 45 ± 16 MPa of the 0.5 μm-diameter pillars to virtually 0 of the 3 μm-diameter ones. This suggests that both dislocation accumulation and annihilation were operating simultaneously in the composite pillars, and their overall flow behavior is governed by the competition of the two. The smooth stress vs. strain response of the largest pillar size group (D = 3 μm) suggests that at this length scale the surface-dominated deformation mechanism was overcome by ones corresponding to the bulk behavior.

Concomitant with the change in burst sizes over different pillar diameters, the strain hardening rates also manifested substantial variation among different pillar size groups, which were obtained by linearly fitting the peak stresses during each burst [7]. The strain hardening rate of the 0.5 μm-diameter pillars was found to be relatively low (902.3 ± 519.2 MPa), while those of the 1 μm-, 1.5 μm- and 2 μm-diameter pillars were much higher. An exceptional case is the 3 μm-diameter pillars which suffered from quick strain softening after yielding.

Fig. 2 shows the representative pre- and post-compression SEM images of the composite pillars with different diameters. Appreciable lateral bulge was observed in all sample sets, indicating that the pillars went through palpable plastic deformation upon compression. Localized shear fracture was found to be the governing failure mechanism of the smallest and largest size groups (0.5 μm- and 3 μm-diameter pillars), while, in stark contrast, most (>70%) of the pillars having intermediate sizes (1 μm-, 1.5 μm- and 2 μm-diameter) tested in this study only showed deformation that was preferentially concentrated at the pillar top. This is in line with the observation in Fig. 1(a) that the compressive flow of the 0.5 μm- and 3 μm-diameter pillars was subject to a

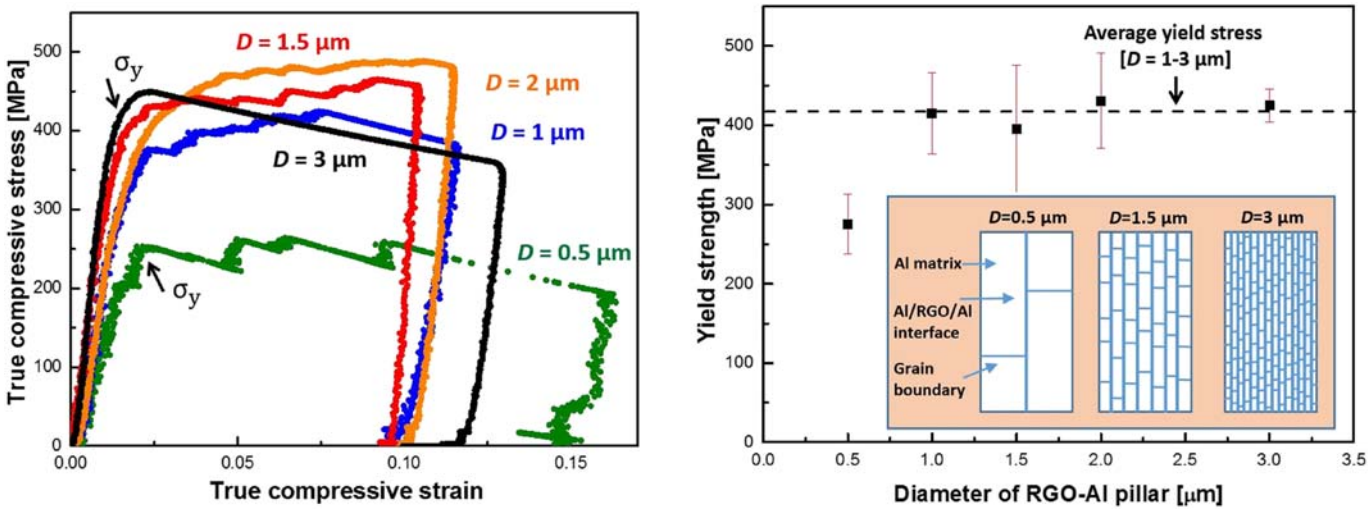

Fig. 1. (a) Representative compressive true stress–strain curves for RGO–Al nanolaminated micro-pillars with varying diameters; (b) Variation of pillars' yield strengths as a function of their diameter. The average yield strengths for pillars of D = 1 μm, 1.5 μm, 2 μm and 3 μm (~410 MPa) is indicated by a dotted line. The inset schematically demonstrates the microstructures of the composite pillars with different diameters.